

## DETERMINATIONS OF P, S-WAVE VELOCITIES AND PORE WATER PRESSURE BUILDUP WITH B-VALUE FOR NEARLY SATURATED SANDS

Sei-Hyun Lee<sup>1</sup>, Yun-Wook Choo<sup>2</sup>, Jun-Ung Youn<sup>3</sup>, and Dong-Soo Kim<sup>4</sup>

### ABSTRACT

Liquefaction resistance depends strongly upon the degree of saturation, which is expressed in terms of the pore pressure coefficient,  $B$ . The  $B$ -value has been widely used to quantify the state of saturation of laboratory samples. However, it is practically impossible to determine in situ state of saturation by using the  $B$ -value. So,  $P$ -wave velocity can be alternatively used as a convenient index for the in situ saturation state.

In this paper, the Stokoe type torsional shear (TS) testing system was modified to saturate a specimen, with which it is also possible to measure the  $P$  ( $V_p$ ),  $S$ -wave velocity ( $V_s$ ) and excess pore water pressure buildup in order to examine the effect of the  $B$ -value for nearly saturated sands. A series of tests were carried out at 3 relative densities (40%, 50% and 75%) and various  $B$ -values using Toyoura sand.

Based on the measurement of the  $V_s$ ,  $V_p$ , while the values of  $V_s$  remains almost constant with an increase of the  $B$ -value, the ratio of  $V_p/V_s$  tends to increase significantly with an increase of the  $B$ -value and the test results are shown to be in good coincidence with theoretically derived formula. The non-dimensional pore water pressure ratio,  $du/\sigma'_0$  also tends to increase and cyclic threshold shear strain,  $\gamma_{th}^c$  which starts the pore pressure buildup by cyclic loading, decreases with an increase of  $B$ -value.

Keywords:  $B$ -value,  $S$ -wave velocity,  $P$ -wave velocity, Torsional shear (TS) test, Pore water pressure

### INTRODUCTION

It has been observed that the liquefaction resistance of sand increases significantly with a decrease in the degree of saturation. According to the studies by Yoshimi et al. (1989), the liquefaction resistance at 70 percent saturation is about 3 times that at full saturation and when the  $B$ -value drops to a level of close to zero at the degree of saturation,  $S_r$ , of about 90%, the liquefaction resistance has been shown to increase roughly 2 times as much as that of fully saturated conditions.

It has been presented by recent studies that in-situ sand is partially saturated despite the deposit is located at several meters below a water table. Kokusho (2000) and Tsukamoto et al.(2002) have reported that  $V_p$  of in-situ soils below a water table is lower than about 1500m/s which is  $V_p$  in pure water, and has the values of 800m/s to 1300m/s despite the soil is located below a ground water table.

<sup>1</sup> Ph. D. Candidate, Department of Civil & Environmental Engineering, KAIST, Daejeon, Korea, Email: [crazyisei@kaist.ac.kr](mailto:crazyisei@kaist.ac.kr)

<sup>2</sup> Post-Doctoral Fellow, Department of Civil & Environmental Engineering, KAIST, Daejeon, Korea.

<sup>3</sup> Ph. D. Candidate, Department of Civil & Environmental Engineering, KAIST, Daejeon, Korea.

<sup>4</sup> Professor, Department of Civil & Environmental Engineering, KAIST, Daejeon, Korea.

This means that the soil deposit several meters below the water table may be not fully saturated but partially saturated soil and the liquefaction resistance may be greater than the value normally evaluated at the fully saturated condition in design practice. Therefore, the effect of the degree of saturation on the undrained behavior of sand and the evaluation of the degree of saturation for in-situ soil may have an important role in geotechnical earthquake engineering.

In laboratory tests, the B-value has been widely used to quantify the state of saturation, because this value is easily measured and accurate enough to indicate partial saturation. It is well known that the pore water pressure coefficient, B, introduced by Skempton (1954) is given as

$$B = \Delta u / \Delta \sigma \quad (1)$$

where  $\Delta \sigma$  and  $\Delta u$  are the increments of the confining cell pressure and the pore water pressure caused by  $\Delta \sigma$  in undrained condition. However, it is practically impossible to monitor the B-value in the field to evaluate the state of saturation of soil.

Nowadays, the velocities of the shear wave,  $V_s$ , and the compressive wave,  $V_p$ , have been measured at a lot of field sites for site investigation by field seismic tests such as the down-hole, cross-hole, up-hole tests and so on. The  $V_p$  is very sensitive to the state of saturation of soil because the compressibility of water is relatively larger than that of soil skeleton (Kokusho, 2000; Tamura et al., 2002; Tsukamoto, 2002). Therefore, the  $V_p$  can be used as a convenient index for the evaluation of saturation. Also, the measurement of  $V_p$  has many advantages in order to make a relation between  $V_p$  and saturation and understand the undrained behaviors of partially saturated sand.

The first objective of this paper is to develop the testing system to make a soil specimen saturated and to perform undrained tests with pore water pressure measurements and, at the same time, to measure the S-wave velocity ( $V_s$ ) and P-wave velocity ( $V_p$ ). The Stokoe-type torsional shear (TS) equipment was modified to saturate a soil specimen and measure the excess pore water pressure buildup ( $\Delta u$ ) during undrained TS tests. Also, the measurement system of the S-wave velocity ( $V_s$ ) and P-wave velocity ( $V_p$ ) was added to the modified TS system. The second objective is to measure the values of  $V_p/V_s$  at various B-values and to compare the  $V_p/V_s$  with a existing theoretical formula. The last objective is to study the effect of partial saturation on the pore water pressure buildup ( $\Delta u$ ) on sand during undrained TS tests.

## MODIFICATIONS OF TORSIONAL SHEAR (TS) TESTING SYSTEM

The Stokoe-type torsional shear (TS) testing system has been widely used to investigate deformational characteristics expressed in terms of shear modulus (G) and damping ratio (D) of soils at shear strains from  $10^{-4}\%$  to 0.1%. The bottom of a soil specimen is rigidly fixed against rotation at a base pedestal while the top (free end) is connected to a drive system that is used to excite and monitor motion as shown in Figure 1. A cyclic torsional force of a given frequency, generally below 10Hz, is applied to the top of the specimen. The stress-strain hysteresis loop is determined from measuring the angle of twist while the voltage applied to the drive coil is calibrated to yield torque. The shear modulus (G) and equivalent damping ratio (D) are calculated from the slope and area of the hysteresis loop, respectively (Kim, 1991).

In this study, the existing Stokoe-type TS testing system was modified to saturate the specimen and to determine the  $V_p$ ,  $V_s$  and excess pore water pressure buildup during undrained TS tests. The schematic configuration of the modified TS testing system is shown in Figure 1.

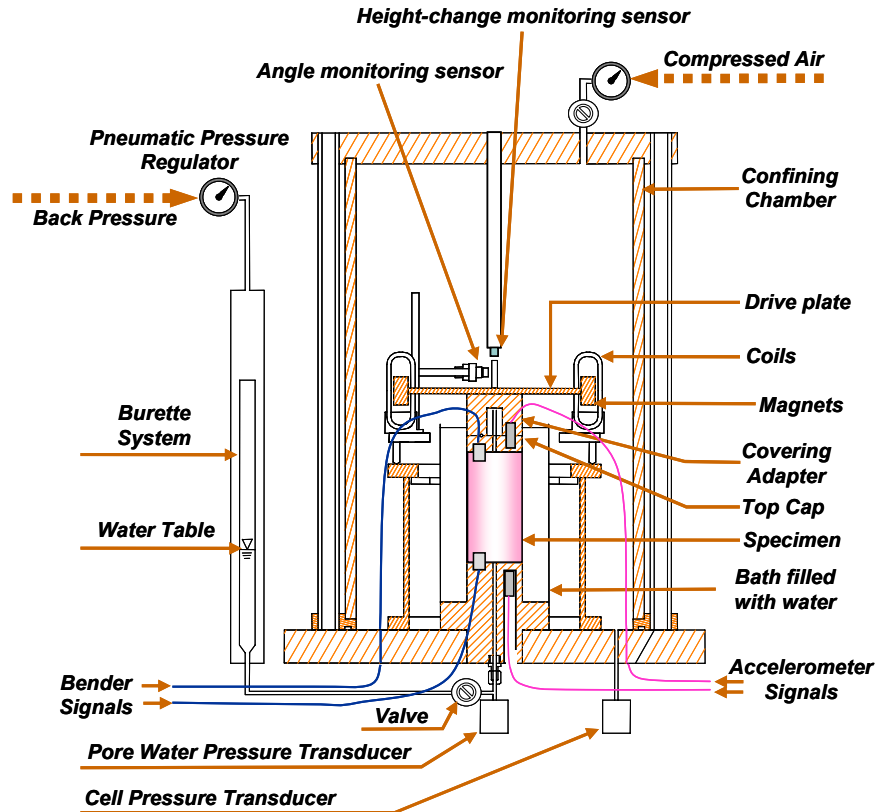


Figure 1. Schematic Configuration of the Modified TS Testing System

### Saturation of Soil Specimen and Measurement of Pore Water Pressure

The modification of TS testing system includes two new elements, which are 1) a quick connector (Swagelok SS-QM2-D-2PM: male part, SS-QM2-B-200: female part) attached to a top cap (Figure 2) and 2) a back pressure system which consists of a pneumatic pressure regulator (Fairchild M 10 regulator), a burette system and a pore water pressure transducer (RDP FDW 150psi) installed at bottom pedestal as illustrated in Figure 1.

First, the quick connector can easily connect and disconnect the pressure lines and when disconnected, the male, female and the corresponding pressure lines are closed. After the preparation of the soil specimen, the tube lines are connected to circulate  $\text{CO}_2$  gas and water through the specimen using the quick connector (Figure 2). After saturation, the quick connector is disconnected and closed.

Second, a back pressure system makes pore water pressure high enough to diminish the size of air bubbles in the pore of the specimen and dissolve air bubbles in water. A pore water pressure transducer measures the back pressure and excess pore water pressure generated during undrained tests. A burette system converts pneumatic pressure to water pressure and transmits pressure to pore water in the specimen. Also, the burette system measures volume changes in the specimen after consolidation and shear loadings.

### Measurement of S-wave Velocity ( $V_s$ )

Bender element (BE) method is a simple technique that determines small-strain shear modulus ( $G_{\max}$ ) of a soil by measuring  $V_s$  through a soil specimen. It is non-destructive, allows for unlimited number of tests and can be set up in most laboratory apparatus. The BE used in this study is produced by Morgan-Electroceramics and made of Lead Zirconate Titanates (PZT 5H) with the following dimensions: 12.7 mm in length, 8 mm in width and 0.7 mm in thickness. The BE is electrically connected with the series-type and coated with waterproofing material (polyurethane). The BE are placed in the slots of a top cap and a bottom pedestal with a protrusion length of about 4mm and each

gap of the slots is filled with epoxy. Finally the BE receiver is covered with conductive coating in order to avoid electromagnetic coupling and cross-talk (Santamarina et al., 2001).

A HP Function Generator Model 33120A is used to supply input signal to the BE of the top cap. Both the input and received signals are averaged 128 times using a smoothing technique by an oscilloscope (HP 54624A) and any filter and amplifier is not used.

### Measurement of P-wave Velocity ( $V_p$ )

In this study, a high frequency accelerometer (PCB 353B16) is used to determine the  $V_p$  through the soil specimen. It is a small size type with the following dimensions 14.5mm in height, 7.1mm in width and 1.5g in weight. The accelerometer has a resonant frequency of 70kHz and an operating range for measurement from 0.7Hz to 18000Hz, so very suitable to measure high frequency vibration accurately. Two accelerometers are mounted in the top cap and bottom pedestal with the BE as shown in Figure 3. The signals from accelerometers are measured by the same oscilloscope (HP54624) used for the BE test.

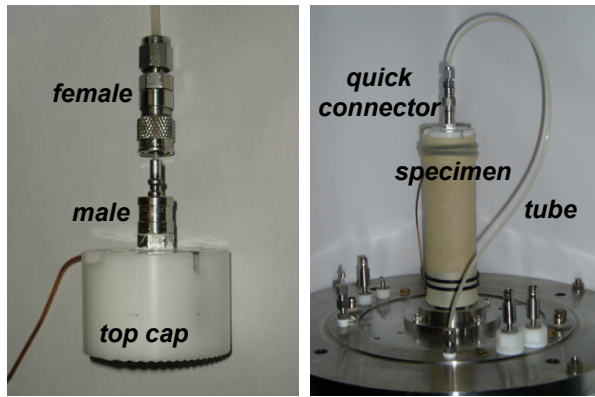


Figure 2. Picture of Quick Connector

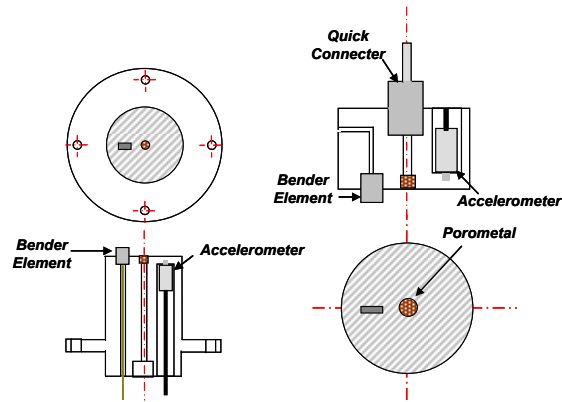


Figure 3. Modified Top Cap and Bottom Pedestal

To transmit the P-wave through the soil specimen, a steel ball of 2mm in diameter is used as a source. P-wave was propagated through the soil specimen as the steel ball impacts on the bottom pedestal. The  $V_p$  is determined by time difference of the first arrival from each accelerometer. However, the time difference has to be corrected using eq. (2), where the calibration coefficient ( $t_c$ ) means time delay caused by the bottom pedestal and top cap because of indirect contact. The  $t_c$  is determined by measuring the time difference from accelerometers when the top cap and bottom pedestal are in direct contact without soil specimen, and has a constant value of about 0.0000285sec (28.5us) in a series of tests.

$$\Delta t = \Delta t_{measured} - t_c \quad (2)$$

### Height Change Monitoring System

The height change of the soil specimen is measured in order to account for the changes in the specimen length during consolidation or swell. Because the change of the specimen length is directly related to the wave propagation length in determining  $V_s$  and  $V_p$ , the measurement of the height-change is very important. Also, the measurement of height-change is used to calculate change in the mass density and void ratio. The height-change monitoring system consists of a proximity transducer (Bently Nevada 3300XL) and an aluminum target installed on top of the target for motion monitoring sensors as shown in Figure 1. The output from the proximity transducer is read with a digital voltmeter and the height change is calculated from the output voltage combined with the calibration factor.

## EXPERIMENTAL SETUP

### Test Material

The test material is Toyoura sand from Japan, widely used in geotechnical laboratory tests. Toyoura sand is classified as poorly graded clean sand without fines. The grain size distribution of test material is shown in Figure 4 and the physical soil properties are summarized in Table 1.

**Table 1. Physical soil properties**

Properties	Toyouura Sand
Unified Soil classification (USCS)	SP
Maximum Void Ratio ( $e_{\max}$ )	0.98
Minimum Void Ratio ( $e_{\min}$ )	0.62
Specific Gravity ( $G_s$ )	2.65
Curvature Coefficient ( $C_c$ )	1.00
Uniformity Coefficient ( $C_u$ )	1.29
Plasticity Index (PI)	NP
Median Particle Size ( $D_{50}$ ), mm	0.20

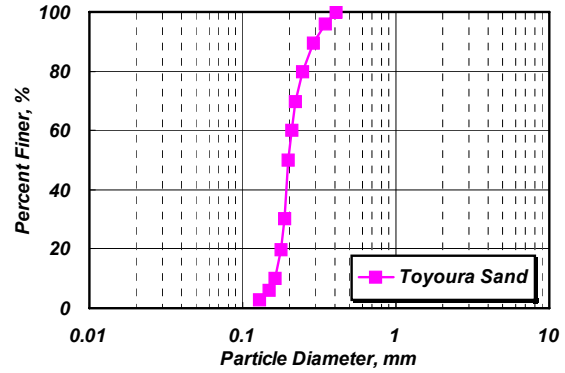


**Figure 4. Grain size distribution of Toyoura sand**

### Test Procedures

Sand specimens of 50mm in diameter and 100mm in height are prepared by air-pluviation method in which air-dried sand is poured in a mold using a nozzle with a rectangular inner cross-section of 1.5 mm×10.0 mm, while maintaining a constant drop-height throughout the preparation, and an initial void ratio  $e_i$  of the sand is controlled by the drop-height. Before the mold is disassembled, vacuum pressure of 20kPa is applied to keep the specimen standing since all tests are performed under effective isotropic confining pressure,  $\sigma'_{o'}$ , of 30kPa in this study. In the case of test with a high B-value above 0.8, CO<sub>2</sub> gas is flowed to expel air through soil specimen by means of a low pressure difference between top and bottom of specimen, less than 15kPa for about 15~30min. Then de-aired water is circulated in order to dissolve CO<sub>2</sub> gas and fill specimen with the water. In the case of test with a low B-value, CO<sub>2</sub> gas is not flowed but the only water is circulated through the specimen. After the circulation, an initial specimen diameter and height were measured and then TS testing system is setup.

**Table 2. Testing Conditions and Procedures**

Material	Toyouura Sand								
Sample Preparation	Air-Pluviation → (CO <sub>2</sub> Circulation) → Water Circulation								
Tests	S-wave velocity (Bender Element)	Input Signal			Square Wave (10kHz)				
		# of Stacks			128				
	P-wave velocity (Accelerometer)	Source			Steel Ball (diameter=2mm)				
		# of Stacks			10				
	Undrained Torsional Shear (TS) Test	Excitation Types			Sinusoidal				
		Loading Frequency			0.5Hz				
		# of Loading Cycles			11				
		Shear Strain Range			$2 \times 10^{-4}\%$ ~0.1% or more				
$\sigma'_{o'}=30\text{kPa}$	$D_r$ (%)	39.8	40.0	44.0	43.5	39.9	39.7	42.0	-
	B-value	0.24	0.32	0.40	0.60	0.69	0.80	0.97	-
	$D_r$ (%)	52.4	48.9	49.6	47.6	50.9	52.2	53.0	50.6
	B-value	0.01	0.28	0.40	0.67	0.83	0.90	0.97	0.99
	$D_r$ (%)	75.6	79.0	76.3	76.6	76.5	74.7	-	-
	B-value	0.16	0.36	0.46	0.56	0.77	0.93	-	-
Sample Preparation → Back Pressure, Cell Pressure → Checking B-value → Measurement of $V_s$ & $V_p$ → Undrained TS Test									

\* $D_r$  means relative density.

The B-value of soil specimen is controlled by increasing the back pressure step by step increments of 50kPa with keeping  $\sigma'_0$  of 30kPa constantly. After applying the back pressure for about 60min, the B-value is measured. When the B-value reaches the target value, both changes of specimen height and volume are measured, and then  $V_s$  and  $V_p$  are determined by the BE and accelerometers, respectively. Finally, the TS test is performed up to 11 cycles at a loading frequency of 0.5Hz under undrained condition. Shear modulus, Damping Ratio and excess pore water pressure are measured in a strain range of 0.0002%~0.1% or more by adjusting an input excitation voltage. The excess pore water pressure generated during the undrained cyclic loading is drained after 11 loading cycles and then next TS test is continued with increasing strain amplitude. The overall testing conditions and procedures are tabulated in Table 2.

## TEST RESULTS

### Variations in $V_s$ with B-value

The typical signals of input and received waves captured in the BE test are shown in Figure 5. Because of almost saturated condition ( $B=0.97$ ), the received waveform shows the effect of the compression wave propagated through the pore water before the shear wave arrives.

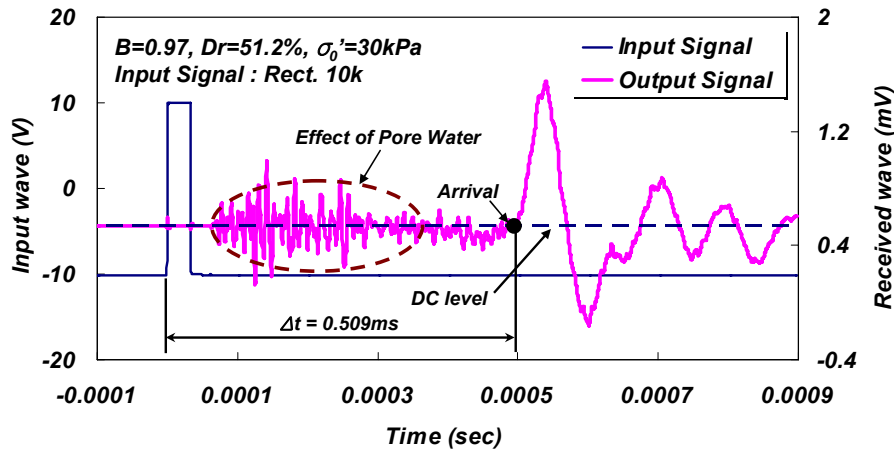


Figure 5. Typical Signals and Determination of Initial Arrival of S-wave in BE tests

In the BE tests, the  $V_s$  is calculated directly by measuring travel distance and travel time. It has been generally confirmed that the travel distance is the distance between tips of two bender elements (Viggiani and Atkinson, 1995). However, there has been much uncertainty in the determination of the travel time. In this study, the travel time was determined as time difference between the start of input signal and the first arrival of the shear wave in the received signal. The first arrival of the shear wave is selected by the following procedure for simplicity and objectivity. The DC level of the received signal is measured by averaging the preceding parts that are not affected by any arrived waveform, and then the arrival time of the shear wave is determined as the time of the cross point where the voltage of the main arrived the shear wave intersects the DC level voltage for the first time as shown in Figure 5 (Kim et al., 2005).

For each relative density,  $D_r$  (40%, 50%, 75%), the variation in the  $V_s$  with the B-value and the mean value of  $V_s$  are presented in Figure 6a. As observed in Figure 6a, there is little difference among the  $V_s$  values with the B-value, showing a maximum difference of about  $\pm 2.5\%$  relative to mean value at each relative density. On the other hand, it is evident that the  $V_s$  values increase as the  $D_r$  increases. In order to eliminate the effect of void ratio and evaluate only that of B-value, the  $V_s$  values are normalized by  $\sqrt{F(e)}$ , which  $F(e)$  is a void ratio function suggested by Hardin(1963) and the variation in  $V_s / \sqrt{F(e)}$  measured in this study with the B-value is presented in Figure 6b. The

$V_s / \sqrt{F(e)}$  is almost constant irrespective of the B-value for  $B \leq 0.6$ . At  $B > 0.6$ , it is also evident that the  $V_s / \sqrt{F(e)}$  decrease slightly as the B-values increase.

$$F(e) = \frac{(2.17 - e)^2}{1 + e} \quad (3)$$

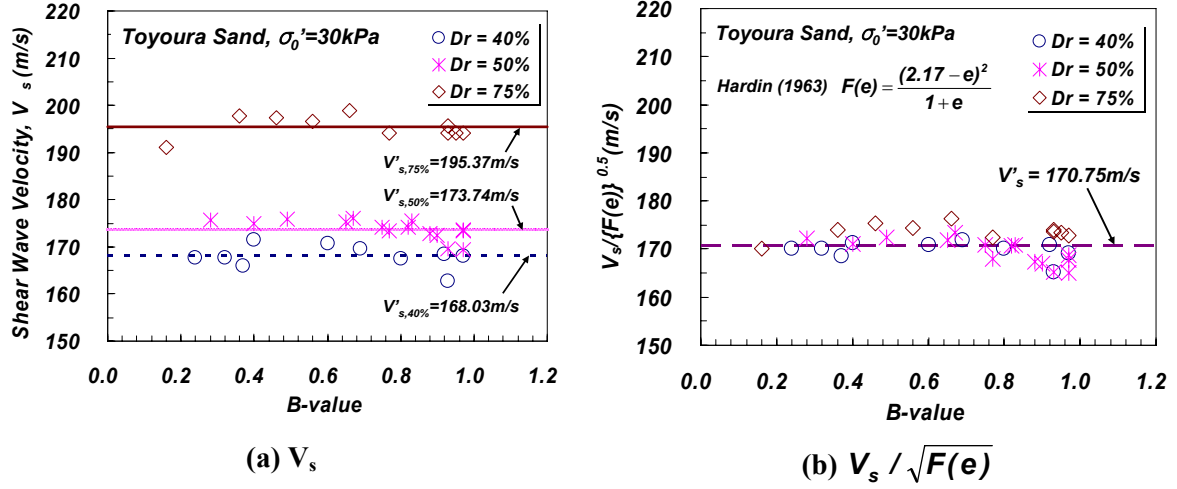


Figure 6. Variations of  $V_s$  and  $V_s / \sqrt{F(e)}$  with B-value and  $D_r$

#### Variations in $V_p$ with B-value

The typical signals captured from the accelerometers to determine  $V_p$  of the specimen are shown in Figure 7. The first arrival of each signal is determined by the same method as that of S-wave. The time difference ( $\Delta t_{\text{measured}}$ ) between the first arrivals of the accelerometers is corrected to determine the travel time ( $\Delta t$ ) of P-wave as indicated in eq. (2).

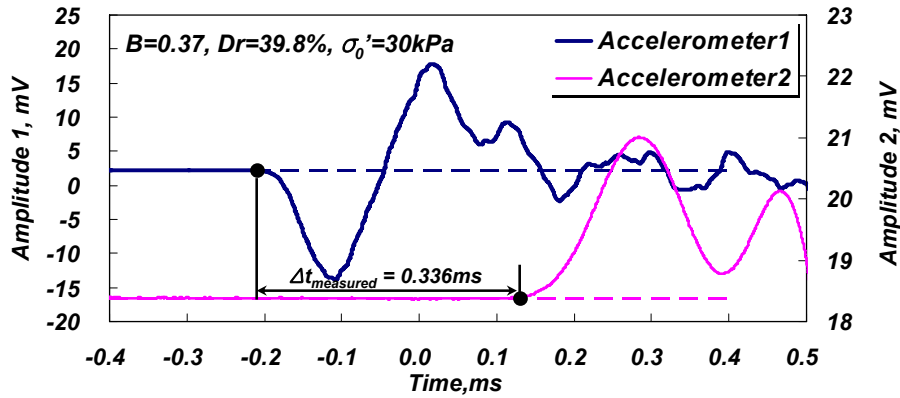


Figure 7. Typical Signals of P-wave from Two Accelerometers

Small amounts of air bubbles in pore water reduce the bulk modulus and wave-propagation velocity of air-water mixture significantly since the compressibility of air is much smaller than that of water. By including the air bubble of 0.1 percent in the air-water mixture, the bulk modulus and wave-propagation velocity of the mixture are reduced by a factor of about 16 and 4, respectively (Richart et al., 1970). Based on the wave propagation theory through a poro-elastic medium, Kokusho(2000) and Tsukamoto et al.(2002) proposed theoretical formulas for determining the  $V_p$  with the B-value on nearly saturated sand as indicated in eq. (4). The theoretical formula, eq. (4) is a relation expressing the velocity ratio  $V_p/V_s$  in terms of the skeleton Poisson's ratio  $\nu_b$  and B-value.



$$\left(\frac{V_p}{V_s}\right)^2 = \frac{4}{3} + \frac{2(1-\nu_b)}{3(1-2\nu_b)(1-B)} \quad (4)$$

Figure 8a presents the  $V_p/V_s$  calculated from eq. (4) for four different values of the skeleton Poisson's ratio and the test results obtained from the modified testing system. As shown in this figure, the test results are shown to be in good coincidence with the theoretical formula and the  $V_p/V_s$  tends to increase apparently with small change of the B-value between  $B=0.8$  and  $B=1.0$ . The degree of saturation ( $S_r$ ) is more than 99.9% for  $B=0.8$ . As stated above, it is verified that the  $V_p$  is very sensitive to the small amounts of the air bubbles in the pore water. It can be also noted that an increase of the  $D_r$  reduces  $V_p/V_s$  a little for  $B \geq 0.6$ , whereas the  $V_p/V_s$  is independent on the  $D_r$  for  $B < 0.6$ . Looking over the whole sets of the test data shown in Figure 8a, it would be reasonable to assume that  $\nu_b = 0.40$  under an isotropic effective stress,  $\sigma'_0 = 30\text{kPa}$ . On the other hand, Tsukamoto et al.(2002) concluded that the skeleton Poisson's ratio is chosen as  $\nu_b = 0.35$  irrespective of the  $D_r$  and  $\sigma'_0$ . However, the Poisson's ratio is related to the shear modulus according to Ishihara (1996). It is expected that the  $\nu_b$  may be affected by the  $D_r$ ,  $\sigma'_0$ , soil type and so on. Further tests are required for various  $D_r$  and  $\sigma'_0$ .

Applying the average values of the  $V_s$  determined from the bender element tests to eq. (4), the theoretical curves of the  $V_p$  for  $D_r=40, 50$  and  $75\%$  are plotted with the test results of  $V_p$  and  $V_s$  in Figure 8b ~ Figure 8d.

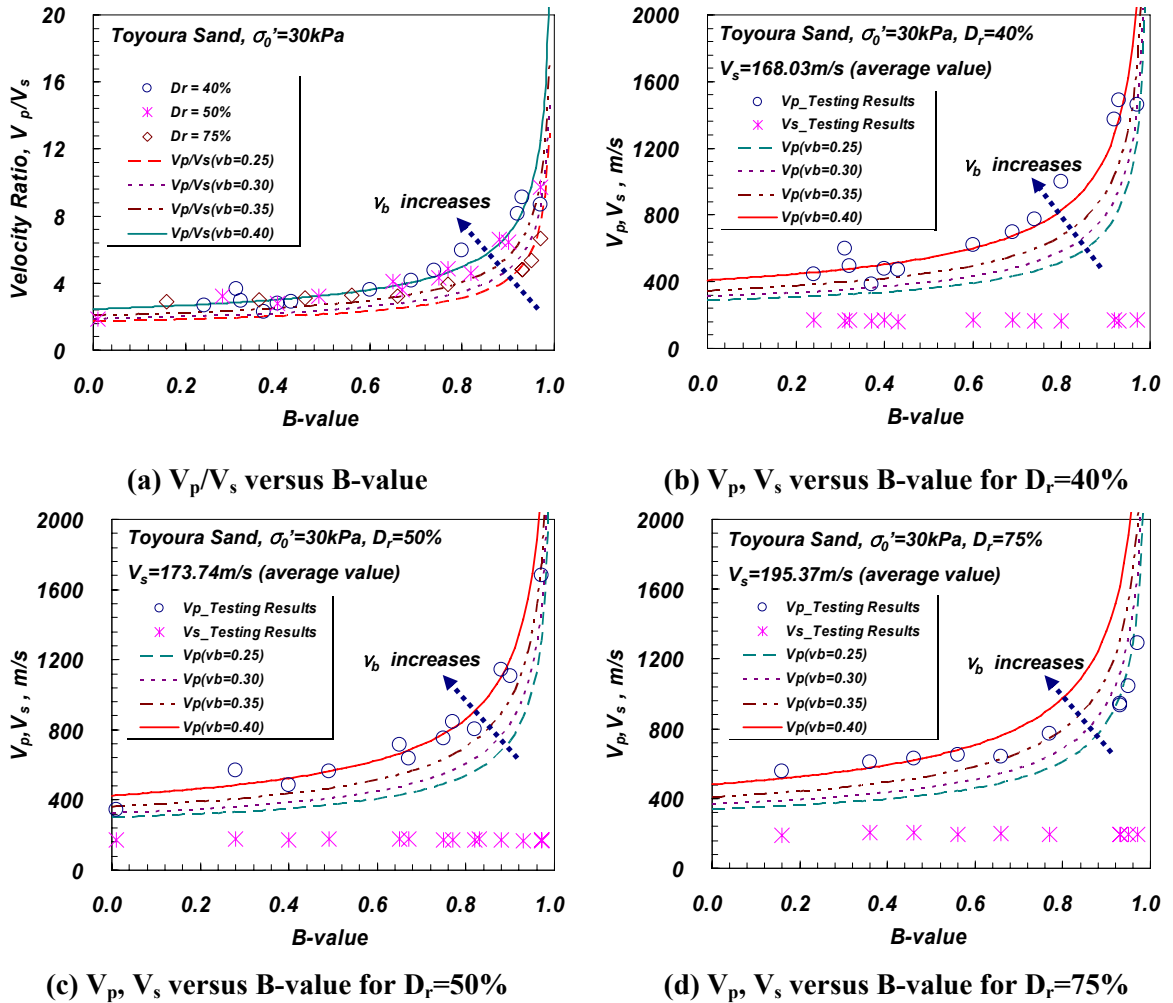
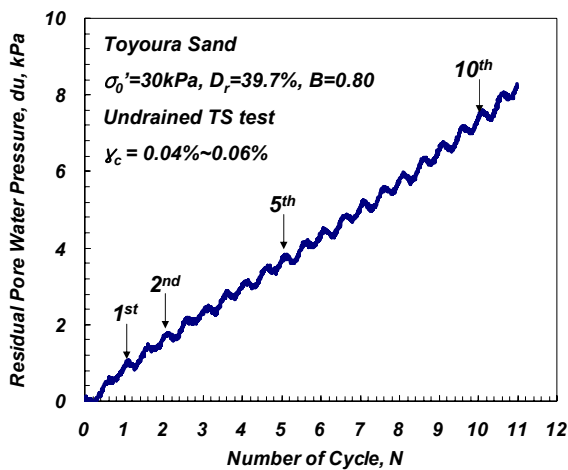


Figure 8. Variations of  $V_p/V_s$ ,  $V_p$  and  $V_s$  with B-value

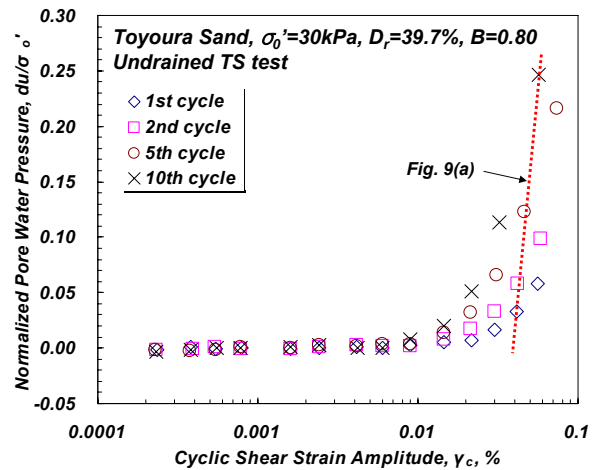


### Variations in Normalized Pore Water Pressure ( $du/\sigma'_0$ ) with B-value

As cyclic loadings apply to a soil specimen in undrained tests, cyclic softening occurs due to the increase of the excess pore water pressure and the shear modulus decreases rapidly. This pore water pressure is called the residual cyclic pore water pressure and is denoted by  $du$  in this paper. The typical residual cyclic pore water pressure buildup with the number of loading cycles (N) at strains of 0.04%~0.06% is plotted in Figure 9a. It can be expected that the residual pore water pressure will reach an initial effective stress of 30kPa if loading cycles are continued. The variations in the normalized pore water pressure,  $du/\sigma'_0$ , which is the residual cyclic pore water pressure normalized by the effective confining pressure, with the cyclic shear strain amplitude,  $\gamma_c$  are plotted in Figure 9b. It can be noted that no residual pore water pressure buildup occurs at strains below approximately 0.01% which called cyclic threshold shear strain ( $\gamma_{th}^c$ ).

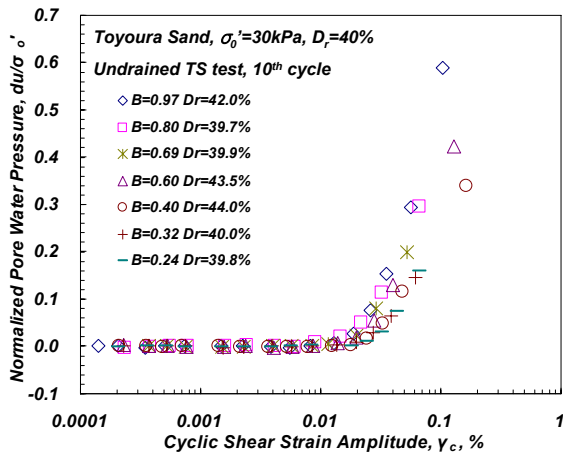


(a) Typical Variation in  $du$  with N

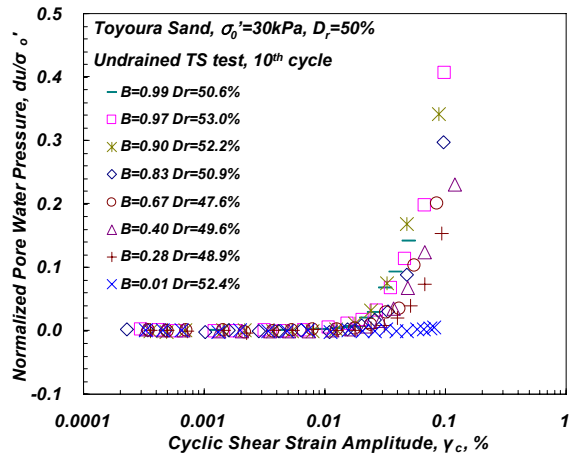


(b) Typical Variation in  $du/\sigma'_0$  with  $\gamma_c$

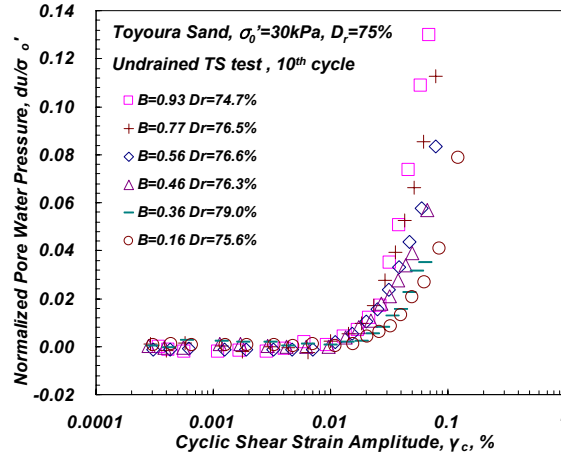
Figure 9.  $du$  and  $du/\sigma'_0$  measured in Undrained TS tests



(a)  $D_r = 40\%$



(b)  $D_r = 50\%$



(c)  $D_r = 75\%$

Figure 10.  $du/\sigma_0'$  versus  $\log \gamma_c$  with various B-values

After 10 loading cycles, the variations in  $du/\sigma_0'$  versus  $\log \gamma_c$  with the various B-values for  $D_r=40, 50$  and  $75\%$  are plotted in Figure 10a through 10c. As the B-value increases, the  $du/\sigma_0'$  increases at a given strain range above the cyclic threshold strain of approximately  $0.01\%$  although there is a little difference in the strain level that the residual pore water pressure buildup starts. In order to observe with the effect of the B-value, the  $du/\sigma_0'$  at a  $\gamma_c$  of  $0.07\%$  is plotted in Figure 11. It is apparently observed that the  $du/\sigma_0'$  increase as the B-value increases and the  $D_r$  decreases. The B-value of about  $0.2$  is equivalent to more than the degree of saturation of  $99\%$  as indicated in Figure 10 (Lade et al., 1977). It is marked that the  $du/\sigma_0'$  increases up to about 3 times by the variation in  $S_r$  which is less than  $1\%$ , comparing the results when the degree of saturation was almost  $100\%$ . In other words, the liquefaction potential of soil is significantly affected by the B-value. In this reason, the effect of the B-value must be considered to estimate the soil behavior in undrained conditions. If the pore water pressure model is to be developed based on the data base obtained from the tests with various types of sand later on, it can be used for a preliminary or rough estimate of the  $du/\sigma_0'$  in field conditions.

#### Variations in Cyclic Threshold Shear Strain ( $\gamma_{th}^c$ ) with B-value

It is shown in the previous section that the  $du/\sigma_0'$  are independent of the number of loading cycles below the cyclic threshold. However, above a certain threshold, the pore water pressure starts to increase with the number of loading cycles. This threshold shear strain is called as the cyclic threshold shear strain. The cyclic threshold shear strain ( $\gamma_{th}^c$ ) can be defined as the cyclic strain amplitude above which volume change occurs in drained and the pore water pressure increases in undrained conditions and/or the modulus and damping values vary with the number of loading cycles during cyclic loading condition. Because the cyclic threshold shear strain is defined as the boundary above which deformation characteristics vary with number of cycles, it is an important factor in the analyses of liquefaction and site response in the field of geotechnical earthquake engineering (Kim, 1991; Vucetic, 1994; Stokoe et al., 1994).

Many researchers have published various results on the existence and characteristics of  $\gamma_{th}^c$ . Kim and Choo (2006) quantitatively defined the  $\gamma_{th}^c$  where the normalized pore water pressure for the  $10^{th}$  cycle,  $du_{10th}/\sigma_0'$ , equals  $0.2\%$  or  $0.5\%$  and investigated extensively the effects of void ratio, effective confining pressure and drainage conditions.

In this study, the  $\gamma_{th}^c$  is defined as shear strain amplitudes, where  $du_{10th}/\sigma_0'=0.5\%$  and based on the test results in Figure 10, the variations in the  $\gamma_{th}^c$  with the B-value for each  $D_r$  are plotted in Figure 12. The  $\gamma_{th}^c$  decreases markedly as the B-value increases, which ranges between  $0.008\% \sim 0.027\%$ . However, it is seen that the  $\gamma_{th}^c$  is almost independent on the  $D_r$  as discussed by Dobry et al. (1982).

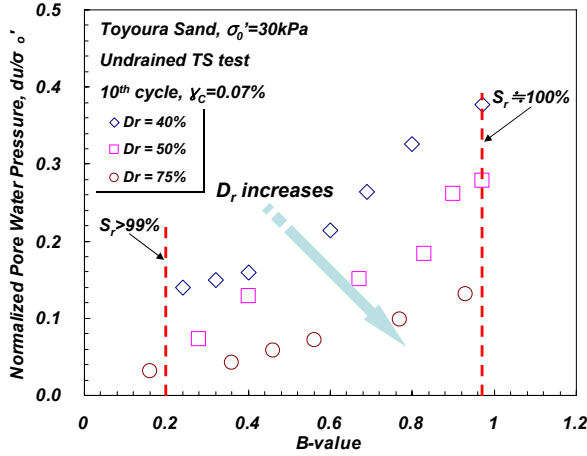


Figure 11.  $du/\sigma'_0$  with B-value at  $\gamma_c=0.07\%$

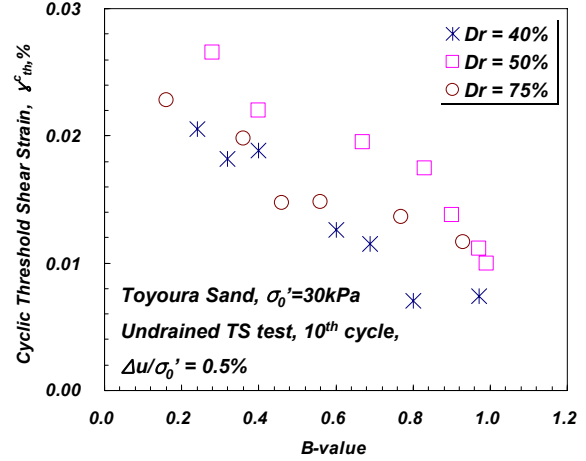


Figure 12. Variations in  $\gamma_{th}^c$  with B-value

## CONCLUSIONS

In this study, the existing Stokoe-type torsional shear (TS) testing system was modified to saturate a soil specimen and determine the  $V_s$  (BE),  $V_p$  (accelerometer) and pore water pressure of nearly saturated sands during undrained TS tests. Toyoura sand was tested at a confining stress of 30kPa but various B-values for 3 relative densities ( $D_r=40, 50$  and  $75\%$ ) and the following observations are made from test results:

- (1) The  $V_s$  is almost constant irrespective of the change of the B-values while the values increase apparently with an increase of  $D_r$ . The values of  $V_s / \sqrt{F(e)}$  eliminated the effect of void ratio decrease slightly as the B-value increases for  $B > 0.6$  but is almost constant for  $B \leq 0.6$ .
- (2) The  $V_p/V_s$  tends to increase apparently with small change in the B-value between  $B=0.8$  and  $B=1.0$ . The  $V_p/V_s$  with the B-value shows good coincidence with the theoretical formulas derived by Kokusho (2000) and Tsukamoto et al. (2002) and the skeleton Poisson's ratio ( $\nu_b$ ) in these formulas was close to 0.4 under  $\sigma'_0=30\text{kPa}$ .
- (3) As the B-value increased, the pore water pressure ratio ( $du/\sigma'_0$ ) increases at a strain range above approximately 0.01%. Comparing with the  $du/\sigma'_0$  at  $\gamma_c=0.07\%$  in order to observe of the effect of B-value definitely, it is interesting to note that the  $du/\sigma'_0$  increases up to about 3 times by the variation in the  $S_r$  which is less than 1%. With the above reasons, it is emphasized that B-value must be considered to estimate the undrained behavior of soil deposit several meters below the ground water table reliably.
- (4) The cyclic threshold shear strain ( $\gamma_{th}^c$ ) decreases markedly as the B-value increases, which ranges between 0.008%~0.027%, but is almost independent on the  $D_r$ .

## ACKNOWLEDGEMENTS

This study was supported by the fund of Construction Research and Development Program (04 construction kernel A01-08) contributed by Ministry of Construction and Transportation and committed by Korea Institute of Construction and Transportation Technology Evaluation and Planning (KICTTEP).

## REFERENCES

- Dobry, R., Ladd, R.S., Yokel, F.Y., Chung, R.M. and Powell, D. "Prediction of pore water pressure buildup and liquefaction of sands during earthquakes by the cyclic strain method," National Bureau of Standards, Building Science Series 138, Washington. D.C., 1982
- Hardin, B. O. and Richart, F. E. Jr. "Elastic wave velocities in granular soils," *Journal of the Soil Mechanics and Foundations Division, ASCE*, Vol. 89, No. 1, pp. 33-35, 1963
- Ishihara, K. "Soil Behaviour in Earthquake Geotechnics" Oxford University Press Unc., New York, pp. 120-123, 1996
- Kim, D.S. "Deformational Characteristics of Soils at Small to Intermediate Strains from Cyclic Tests," Ph.D. Thesis, University of Texas at Austin, 1991
- Kim, D.S., Choo, Y.W. "Cyclic Threshold Shear Strains of Sands Based on Pore Water Pressure Buildup and Variation of Deformation Characteristics," *IJOPE*, Vol. 16, No. 1, pp. 57-64, 2006
- Kim, D.S., Youn, J.U., Lee, S.H. and Choo, Y.W. "Measurement of Gmax of sands Using Bender Element in Resonant Column and Torsional Shear Equipment," *Journal of Korea Geotechnical Society*, Vol. 21, No. 10, pp. 17-25, 2005 (in Korean)
- Kokusho, T. "Correlation of pore-pressure B-value with P-wave velocity and Poisson's ratio for imperfectly saturated sand or gravel," *Soils and Foundations*, Vol. 40, No. 4, pp. 95-102, 2000
- Lade, P.V. and Hernandez, S.B. "Membrane penetration effects in undrained tests," *Journal of the Geotechnical Engineering Division, ASCE*, Vol. 103, No. GT2, pp. 109-125, 1977
- Richart, F. E. Jr., Hall, J. R. Jr. and Woods, R. D. "Vibrations of Soils and Foundations," Prentice-Hall International, Inc., Englewood Cliffs, NJ, pp. 129-132, 1970
- Santamarina, J. C., Klein, K. A. and Fam, M. A. "Soils and Waves," John Wiley & Sons, LTD, pp. 238-282, 2001
- Skempton, A. W. "The pore pressure coefficients A and B," *Geotechnique*, Vol. 47, pp. 133-147, 1954
- Stokoe, KH, II, Hwang, SK, Lee, JNK and Andrus, RD. "Effects of Various Parameters on the Stiffness and Damping of Soils at Small to Medium Strains," *Proc. of the First Int Conf on Pre-failure Deformation Characteristics of Geomaterials*, Vol 2, pp 785-816, 1994
- Tamura, S., Tokimatsu, K., Abe, A. and Sato, M. "Effects of air bubbles on B-value and P-wave velocity of a partly saturated sand," *Soils and Foundations*, Vol. 42, No. 1, pp. 121-129, 2002
- Tsukamoto, Y., Ishihara, K., Nakazawa, H., Kamada, K. and Huang, Y. "Resistance of partly saturated sand to liquefaction with reference to longitudinal and shear wave velocities," *Soils and Foundations*, Vol. 42, No. 6, pp. 93-104, 2002
- Viggiani, G. and Atkinson, J. H. "Interpretation of bender element tests," *Géotechnique*, Vol. 45, No. 1, pp. 149-154, 1995
- Vucetic, M. "Cyclic threshold shear strains in soils," *Journal of Geotechnical Engineering, ASCE*, Vol. 120, No. 12, pp. 2208-2228, 1994
- Yoshimi, Y., Yanaka, K. and Tokimatsu, K. "Liquefaction resistance of a partially saturated sand," *Soils and Foundations*, Vol. 29, No. 2, pp. 157-162, 1989